

Measurement of the top pair cross section in dileptonic channels with a hadronic tau and branching ratio $t \rightarrow \tau \nu b$, with 9.0 fb⁻¹

The CDF II Collaboration
URL <http://www-cdf.fnal.gov>
(Dated: September 6, 2012)

The top quark pair production and decay into leptons with at least one being a τ lepton is studied in the framework of the CDF experiment at the Tevatron proton antiproton collider at Fermilab (USA). The selection requires an electron or a muon produced either by the τ lepton decay or by a W decay. The analysis uses the complete Run II data set i.e. 9.0 fb⁻¹, selected by one trigger based on a low transverse momentum electron or muon plus one isolated charged track. The top quark pair production cross section at 1.96 TeV is measured at $8.2 \pm 2.3_{-1.1}^{+1.2} \pm 0.5$ pb, and the top branching ratio into τ lepton is measured at $0.120 \pm 0.030_{-0.019}^{+0.022} \pm 0.007$ with statistical, systematics and luminosity uncertainties. These are up to date the most accurate results in this top decay channel and are in good agreement with the results obtained using other decay channels of the top at the Tevatron. The branching ratio is also measured separating the single τ lepton from the two τ leptons events with a log likelihood method. This is the first time these two signatures are separately identified. With a fit to data along the log-likelihood variable an alternative measurement of the branching ratio is made: $0.098 \pm 0.022(stat.) \pm 0.014(syst.)$; it is in good agreement with the expectations of the Standard Model (with lepton universality) within the experimental uncertainties. The branching ratio is constrained to be less than 0.159 at 95% confidence level.

I. INTRODUCTION

The Standard Model (SM) has represented for more than 4 decades the most successful synthesis of the theoretical and experimental studies of particle physics. The model with few modification for accomodating the neutrino mixing has been confirmed by all the experiment to very high precision levels.

Despite its success, the SM contains an inconsistency in the term describing the longitudinal WW scattering. The cross section of this process grows with the momentum exchanged and the unitarity of the SM is violated at the energy scale of the order of TeV. The recently observed Higgs boson will fix this. Several beyond the Standard Model theories incorporate in addition to this Higgs boson new particles and interactions. The interactions may be a consequence of doublets of Higgs fields, that generate physical representations like the charged Higgs boson. These boson states are direct deduction of SM extensions like supersymmetric models. The minimal formulation of these models, the Minimal Supersymmetric Standard Model (MSSM), requires at least two Higgs doublets that imply the existence of a pair of charged Higgs bosons.

Top pair production with decay into tau and a final state containing a hadronic tau decay is one of the least explored processes. A precise measurement of the branching ratio of top quark into tau represents one important tool to test the properties of the SM and search for unobserved mediators that interact with both the top and the tau fields, where the charged Higgs boson is one possible candidate.

The decay process we want to observe is $t\bar{t} \rightarrow b\bar{\tau}\nu + \bar{b}\tau\bar{\nu}$, where one of the tau decays leptonically in an electron or a muon, and the other decays hadronically into a jet of hadrons. We select events which contain missing transverse energy, due to the emission of neutrinos, and at least 2 hadron jets from b quark decay. The analysis presented in this thesis investigats the existence of a charged Higgs boson as direct products of the top quark decay.

This thesis is based on the data collected by the Collider Detector at Fermilab (CDF), located in Fermi National Accelerator Laboratory, Batavia, Illinois. The data was acquired during Run II, that lasted from 2002 through the summer 2011, corresponding to 10.0 fb^{-1} of integrated luminosity.

II. THE CDF DETECTOR

The CDFII detector [1] is a large multipurpose solenoidal magnetic spectrometer, designed with an approximately cylindrically symmetric layout. The detector consists of several specialized subsystems arranged in concentric layers, each one meant to perform a specific task.

The inmost part of CDF tracker is the Silicon detector, composed by three subunits: the Layer 00 (L00) [3], the Silicon Vertex Detector (SVXII) [4] and the Intermediate Silicon Layers (ISL) [5], covering the $|\eta| < 4$ region from 1.35 to 28 cm from the beam pipe. Outside is located an open-cell wire drift chamber, the Central Outer Tracker (COT) [2], which allows a precise measurement of the impact parameter of the particle tracks. The COT contains 96 sense wire layers, which are radially grouped into eight *superlayers*.

The CDF calorimeters [1] covers the region $|\eta| < 3.6$. Central sector of the calorimeter, is divided into the Central Electromagnetic Calorimeter (CEM) and the Central Hadronic Calorimeter (CHA). Plug calorimeter is placed in the region with $1.1 < \eta < 3.6$ and consists of the Plug Electronic Calorimeter (PEM), and Plug Hadronic Calorimeter (PHA). A supplementary calorimeter, the Wall Hadronic Calorimeter (WHA), is located behind the CEM/CHA system and above the plugs.

The muons dectectors [6] have a coverage of $0.03 \lesssim |\eta| \lesssim 1.5$. The system is divided in the Central MUon detector (CMU), the Central Muon uPgrade (CMP), the Central Muon eXtension (CMX), and the Intermediate MUon system (IMU).

Cherenkov Luminosity Counters, CLC [7] measures the instantaneous luminosity. They are located in the forward region of the detector;

III. SAMPLES

We use a trigger class, which are generally denoted as *lepton plus isolated track*. This class selects a CMX or CMUP muon of transverse momentum $p_T \geq 8$ GeV or an electron with a calorimeter transverse energy deposition $E_T \geq 8$ GeV, paired with an isolated track of $p_T \geq 5$ GeV. The isolation requirement imposes no tracks of $p_T \geq 1.5$ GeV to be contained in an isolation annulus ranging from 10° to 30° .

The total integrated luminosity used in this analysis is 9.0 fb^{-1} , requiring the good detector conditions.

IV. PARTICLE IDENTIFICATION

The signature of the processes we want to select contain one electron or one muon, one jet of hadrons induced by a tau decay and two jets of hadrons from the b quark decay.

The neutrinos represent an invisible part of the decay products and their number is three in case the electron (muon) directly comes from the W boson decay or five in case the electron (muon) originates from a tau decay.

A. Electron and Muon Identification

Central electron are characterized by a very narrow energy deposit (“cluster”) in the central electromagnetic calorimeter. The electromagnetic fraction of the energy deposit and the information of the calorimeter shower shape is used to discriminate the background.

Two different muon categories are used in the analysis: central muons reconstructed in the CMU+CMUP and in the CMX detectors. The identification requires a small deposit of energy in the calorimeter and a good match between the track reconstructed by the COT and the muon chamber hits.

For background veto purposes we defined for Minimum Ionizing Particles. This class of particles can be muons which do not pass the standard identification of CMUP or CMX muons because of the inefficiency of the detector or gaps between the elements of the muon detector systems. They are required to pass the same muon requirements on the energy deposit in the calorimeter.

B. Tau Reconstruction and Identification

The offline reconstruction starts with the tagging of “seed” calorimeter towers with transverse energy $E_T^{seedtwr} > 6$ GeV. Then shoulder towers with energy $E_T^{shwtwr} > 1$ GeV are added to form a calorimeter cluster and the number of tower contributing to the cluster, $N^{twr} < 6$.

The identification requires a seed track $p_T^{seedtrk} > 4.5$ GeV/c should be matched to the “seed” tower. The direction of the seed track is then used as reference direction for selecting the offline tau decay products. A cone that contains the tau decay products is defined with a variable amplitude $\theta_{sig} = \min(0.17, 5.0/E^{cluster}[\text{GeV}])$ rad (shrinking cone). The tracks and reconstructed neutral pions in the signal cone are then used to compute the four-momentum of the tau decay products. This is called the visible momentum. An isolation annulus, 30 degrees wide, surrounding the signal cone, collects the reconstructed particles which are used to reject hadron jets misidentified as tau.

The identification requires also the quadri-momentum of the tracks in the signal cone should have an invariant mass $M^{vis} < 1.8$ GeV/c². Moreover a cut is added to remove the contamination from misidentified muons, $E/P > 0.4$, where E represents the cluster energy and P the scalar sum of signal track transverse momenta. The variable ξ' is defined to suppress electrons or muons releasing a large

fraction of electromagnetic energy in the calorimeter. It is defined as:

$$\xi' = \frac{E_{tot}}{\sum |\vec{p}_i|} \left(0.95 - \frac{E_{EM}}{E_{tot}} \right); \quad (1)$$

C. b Quark Identification

Top quarks are expected to always decay into W and b quarks in the SM framework. The mass of the b hadrons is small compared to the momentum, so the products of its decay are emitted as jets. In our analysis we apply the following selection on the jets:

- $\eta \leq 2.0$
- $E_T > 20$ GeV for the leading jet, 15 GeV for the subleading ones.
- $E_{EM}/E < 0.9$

where E_{EM}/E represents the electromagnetic fraction of the jet cluster energy and E_T the jet corrected transverse energy.

We exploit the long lifetime of a b flavoured hadron to identify jets originating from a bottom quark through the presence of a decay vertex displaced from the primary interaction vertex. The SECVTX [15] tag technique operates on a per jet basis. A displaced vertex requires at least two tracks, which passed track quality cuts and have a non negligible impact parameter with respect to the primary vertex.

D. Missing Transverse Energy

The \cancel{E}_T in the event indicates the presence of neutrinos. We obtain the \cancel{E}_T as estimate of the sum of the neutrino momenta. We correct the \cancel{E}_T taking into account:

- the transverse momentum of identified muons and minimum ionizing particles;
- the primary vertex position instead of geometric center of the detector.

V. SIGNAL AND BACKGROUND

A. Signal Events

To guide our selection of $t\bar{t}$ events with single or both top quarks decaying into tau, ν_τ and b , we prepared an artificial sample of $t\bar{t}$ events. Events are generated in the SM picture using Monte Carlo technique with the PYTHIA event generator.

B. Background events

We estimate the physics background using simulated data samples. We rely on the simulation to describe the overall selection acceptance and we apply scale factors to account for small mismodeling.

The events where QCD induced jets are misidentified as tau decay products is the major source of background with fakes. We implemented a technique to evaluate the background with QCD hadron jets faking taus. This methods uses the probability of jets (“fake rate”) to pass the tau identification cuts. The component to the background caused by electrons or muons misidentified as taus is evaluated through simulated data.

C. Background of Jets Misidentified as Taus

The tau fake rate has been computed using jet data samples. They are collected with triggers that require the event to have at least a calorimeter cluster. We reject events which contain an electron or muon candidate, or have an high \cancel{E}_T : $\cancel{E}_T < 20 + \sqrt{\Sigma E_T}$ GeV where ΣE_T is the scalar sum of the calorimeter transverse energy.

We start from the selection of loosely selected jets, which pass the tau reconstruction and we call “fakable tau object”. Their number is the denominator, while the number of fakable tau objects which pass the tau identification is the numerator of the fake rate.

The leading jets have on average higher fake rate than the subleading ones (the second with highest E_T). In this analysis the average between the two results is used to compute the number of expected events with fake tau candidates. The difference is considered as systematic uncertainty of the fake rate measurement. The fake rate is parametrized as function of the E_T and $|\eta|$ of the cluster and on the track multiplicity of the hadron jet.

The results corresponding to data sets collected from April the 18th 2008 until February 25th 2010 are shown in Figure 1, for taus with 1 and 3 tracks. We computed the tau fake rates in data taking

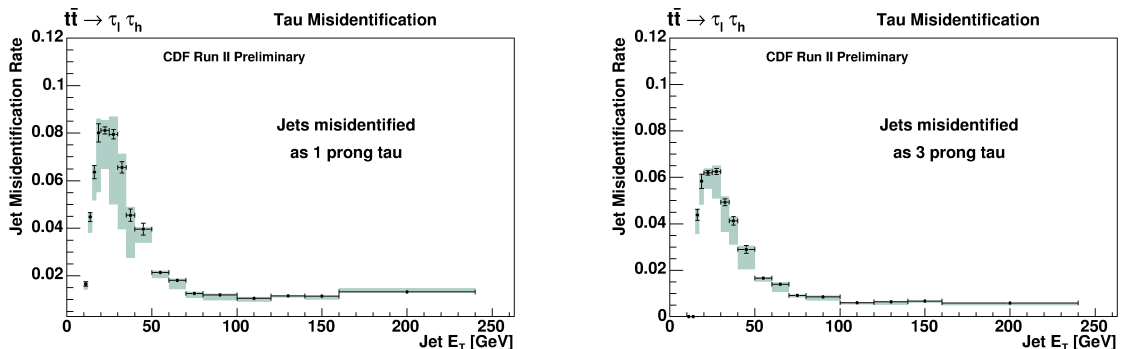


Figure 1: The fake rate for data taken since April the 18th 2008 until February 25th 2010. On the left, the result for 1 prong taus, and on the right, 3 prong taus, the result is the average of the fake rate computed for the leading and subleading jets.

periods corresponding to different regimes of luminosity. The different results are used to estimate the events with fakes selected during the corresponding data taking periods.

D. Data Sample for Background with Fakes

We measure the expected background of events of jets misidentified as tau with single lepton samples. We require exactly one central electrons or muon with $p_T > 8$ GeV. The sample of events with one CMX muon has been selected with the additional trigger requirement of a 5 GeV track.

To estimate the events with fakes we collect events with one electron or one muon candidate paired with at least a fakable tau object. Every fakable tau object is then considered as a possible selected event weighted by the probability of the fakable object to be misidentified. To reject the component with genuine taus we reject events with tau candidates.

E. Electron or Muon Misidentified as Tau

The production of a Z boson, with decay $Z \rightarrow ee/\mu\mu$, represents a source of background, when one of the leptons passes the tau identification requirements. We estimate the expected numbers of background events from this source through Alpgen generated samples.

VI. KINEMATIC SELECTION

We then require:

- exactly 1 tau candidate;
- exactly 1 electron or 1 muon candidate;
- lepton with opposite charge;
- 2 jets;
- missing transverse energy $\cancel{E}_T \geq 10$ GeV;
- $H_T \geq 150$ GeV in case of events with 1 prong taus, $H_T \geq 155$ GeV in case of 3 prong taus, where $H_T = \cancel{E}_T + E_T^{tau} + \sum_i E_T^{jet_i}$, E_T^{tau} is the cluster E_T of the tau decay products, $E_T^{jet_i}$ is the E_T of all the jets passing the jet requirements.

We apply a veto to remove the Drell-Yan processes. We reject the events from the electron sample when any jets with 90% electromagnetic energy fraction, has an invariant mass with the electron candidate compatible with the Z resonance $86 \leq M_{inv} \leq 96$ GeV. We reject events from muons sample when we find any minimum ionizing particle which has an invariant mass with the muon candidate in the ranges $76 \leq M_{inv} \leq 106$ GeV and $M_{inv} \leq 15$ GeV.

VII. SYSTEMATICS

A. Rate Systematics

The CDF experiment measures the luminosity with the Cherenkov Luminosity Counters, CLC. The acceptance of the counters and the inelastic $p\bar{p}$ cross section are the dominant uncertainties in the luminosity measurement. The instantaneous luminosity relative uncertainty is 5.9%.

A source of systematic uncertainty is the uncertainty of the cross section assigned to each physics process estimated with MC samples. The MCFM program [21] has been used to compute the diboson processes cross section (WW , WZ and ZZ) [22]. It has an uncertainty of 6%. The experimental uncertainty of Drell-Yan events is obtained from a recent CDF public result [18], 15%.

B. Uncertainty of Monte Carlo Generator

The parton showering is modelled differently in the PYTHIA and HERWIG MC simulation. The differences are evaluated simply comparing the efficiency measurement obtained with the two generators. We measured the Color Reconnection systematic uncertainty replacing the standard $t\bar{t}$ PYTHIA MC samples with two tuning: Apro and ACRpro. We also estimated the effect with two $t\bar{t}$ PYTHIA MC samples having more Initial State Radiation (ISR) and Final State Radiation (FSR). We determine the systematic uncertainty due to the uncertainty in the PDF's by using different sets: CTEQ5L [20] considered as our standard, MRST72, MRST75, CTEQ6L, CTEQ6L1 and CTEQ6M.

$t\bar{t} \rightarrow \tau_e \tau_h + X$	Events after Kinematic Selection		
	Process	Muon Sample	Electron Sample
Fakes	$35.6 \pm 1.5^{+2.9}_{-7.8}$	$63.9 \pm 3.7^{+5.8}_{-13.5}$	$99.6 \pm 4.0^{+8.7}_{-21.3}$
$Z/\gamma^* \rightarrow \tau\tau$	$43.3 \pm 1.1 \pm 8.8$	$50.6 \pm 1.2 \pm 10.3$	$94.0 \pm 1.6 \pm 19.2$
$Z/\gamma^* \rightarrow \ell\ell$	$3.5 \pm 0.3 \pm 0.7$	$3.5 \pm 0.2 \pm 0.7$	$7.0 \pm 0.4 \pm 1.4$
Diboson	$1.8 \pm 0.2 \pm 0.2$	$2.4 \pm 0.2 \pm 0.3$	$4.2 \pm 0.3 \pm 0.6$
$t\bar{t} \rightarrow \tau\ell + X$	$23.7 \pm 0.1 \pm 2.3$	$30.7 \pm 0.1 \pm 3.0$	$54.5 \pm 0.2 \pm 5.3$
$t\bar{t} \rightarrow \tau\tau + X$	$2.5 \pm 0.0 \pm 0.2$	$3.2 \pm 0.0 \pm 0.3$	$5.7 \pm 0.1 \pm 0.6$
Total Expected	$110 \pm 2^{+11}_{-13}$	$154 \pm 4^{+14}_{-19}$	$265 \pm 4^{+25}_{-32}$
Observed	115	175	290

CDF Run II Preliminary, 9.0 fb^{-1}

Table I: Expected events and data events passing the kinematic selection.

C. b Jet Tag and Energy Scale

The event with a tight SECVTX tag should be reweighted by 96.0% with a systematic uncertainty of 5%. The jets that could be mistagged are weighted by the mistag probability and in this case the systematic uncertainty is about 20%. The total uncertainty is given by the sum over all the events of the systematic uncertainty of the tag and the mistag. We apply a jet energy correction (JEC) to data and MC. We calculate the propagation of the uncertainties applying $\pm 1\sigma$ shifts to the energy scale.

D. Pile Up

The evaluation of the uncertainty of the selection efficiency was done reweighting the MC events on the base of the primary vertex multiplicity. We generated the templates of vertex multiplicity in the signal $t\bar{t}$ MC and in the data. We considered two instantaneous luminosity regimes as lower and upper limits.

E. Tau Related Systematics

The systematics we consider related with the tau lepton selection are three. The first is relative to the fake rate measurement and propagate into the expected number of events with fakes. The second is related to the uncertainty on the scale factors to be multiplied to the estimate from MC. The last systematic uncertainty is the uncertainty in the energy scale of the tau cluster of the hadronic calorimeter towers, shifted by $\pm 5\%$.

VIII. SELECTION RESULT

We apply the selection reported in Section VI and obtain the result summarized in Table I. The comparison of data observed events and the expected ones is in agreement in the statistic uncertainty. Figure 2 show the basic characteristic kinematic distributions of the processes we study, summing over all the lepton categories. The selected events still contain a severe contamination of events with fake taus and the irreducible background due to Drell-Yan processes in two taus.

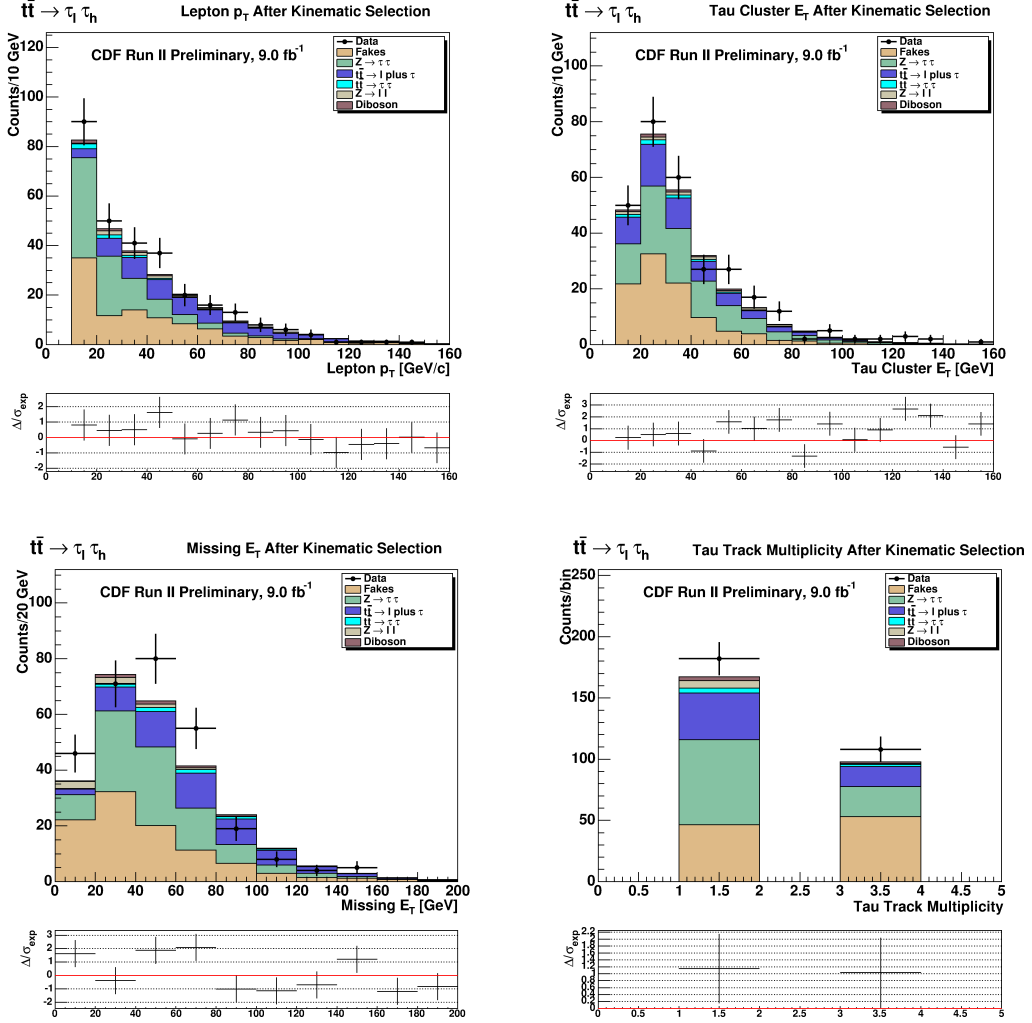


Figure 2: Distribution of electron E_T and muon p_T (top left), of tau cluster E_T (top right), \cancel{E}_T (top left), and track multiplicity of tau induced jet (top right).

A. Secondary Vertex Requirement

To remove the contamination we require one secondary vertex tag from the tight SECVTX algorithm (see Section IV C). We obtain the result summarized in Table II. Figure 3 show the basic characteristic kinematic distributions of the processes we study after the kinematic selection and the request of at least one secondary vertex. The plots are obtained summing over all the lepton categories. We can notice in Figure II that most of the irreducible background is rejected, still a small fraction of Drell-Yan processes in tau is remaining. After the requirement of a tight SECVTX tag still we observe a non negligible expectation from events with fake taus. This stimulated us to investigate further on the source of this background.

$t\bar{t} \rightarrow \tau_\ell \tau_h + X$		Events after b-Tag	
Process	Muon Sample	Electron Sample	Total
Fakes	$5.47 \pm 0.59^{+0.34}_{-0.98}$	$10.78 \pm 1.63^{+0.83}_{-2.29}$	$16.25 \pm 1.74^{+1.17}_{-3.27}$
$Z/\gamma^* \rightarrow \tau\tau$	$1.70 \pm 0.09 \pm 0.37$	$2.17 \pm 0.10 \pm 0.47$	$3.87 \pm 0.14 \pm 0.85$
$Z/\gamma^* \rightarrow \ell\ell$	$0.15 \pm 0.03 \pm 0.04$	$0.12 \pm 0.01 \pm 0.03$	$0.26 \pm 0.03 \pm 0.07$
Diboson	$0.11 \pm 0.02 \pm 0.03$	$0.13 \pm 0.03 \pm 0.03$	$0.24 \pm 0.03 \pm 0.06$
$t\bar{t} \rightarrow \tau\ell + X$	$13.50 \pm 0.96 \pm 1.62$	$17.46 \pm 0.11 \pm 2.10$	$30.96 \pm 0.15 \pm 3.73$
$t\bar{t} \rightarrow \tau\tau + X$	$1.44 \pm 0.03 \pm 0.18$	$1.83 \pm 0.04 \pm 0.23$	$3.27 \pm 0.05 \pm 0.41$
Total Expected	$22.4 \pm 0.6^{+1.7}_{-2.5}$	$32.5 \pm 1.6^{+2.3}_{-3.8}$	$54.9 \pm 1.7^{+3.9}_{-6.3}$
Observed	18	40	58

CDF Run II Preliminary, 9.0 fb⁻¹

Table II: Expected events and data events passing the kinematic selection and the requirement of one tight SECVTX tag.

B. Likelihood Discriminant

Before looking at the event kinematic to search for variables that allow us to distinguish signal and background we need to understand the origin of events with misidentified taus a bit more. To study in more details the dominant contributions in the misidentified tau background we used $t\bar{t}$ and $W + b\bar{b}$ Monte Carlo samples. The study showed us that the largest contribution in the misidentified tau background comes from $t\bar{t}$ production with one W decaying into electron or muon and the other hadronically.

To separate $t\bar{t}$ production in the dilepton decay channel with tau from the main background of misidentified taus, we look for variables that distinguish the two sources. The two tau identification variables most sensitive to misidentified taus are the $E^{Cluster}/p$ and tau isolation, Σp_T^{iso} . We also looked into the kinematic of single lepton $t\bar{t}$ events and identify variables to distinguish them from our signal events. We found the most relevant variables to be:

- the module of the missing transverse energy,
- the transverse mass of the electron plus \cancel{E}_T system, $M_T(e, \cancel{E}_T)$,
- the transverse energy of the third highest E_T jet,

We implemented in our analysis a Likelihood based selection. The method we implement is known as *Log-Likelihood Ratio (LLR)* discriminant: the tool is easily obtained combining one-dimensional distribution templates of background and signal events.

In a multidimensional space, events are represented by vectors $\vec{x} = (x_1, \dots, x_n)$, where the coordinates are the observed variables characterizing it. Supposing two hypotheses, H_0 or H_1 , related to the signal and background processes, the events \vec{x} are distributed with *pdfs* $p_0^i(x^i)$ and $p_1^i(x^i)$, where $i = 1, \dots, n$. We define *LLR* in the following way:

$$\ln(LLR) = \ln \left(\frac{P_0(\vec{x})}{P_1(\vec{x})} \right), \quad (2)$$

where the $P_0(\vec{x})$ and $P_1(\vec{x})$ are defined

$$P_0(\vec{x}) = \prod_{i=1, \dots, n} p_0(x^i), P_1(\vec{x}) = \prod_{i=1, \dots, n} p_1(x^i), \quad (3)$$

The *pdfs* we used are binned distributions. We show in Figure 4 the comparison between data and expectation for the full data sample, before and after the SECVTX tag. The modelling of the data events looks in agreement in the statistic uncertainty.

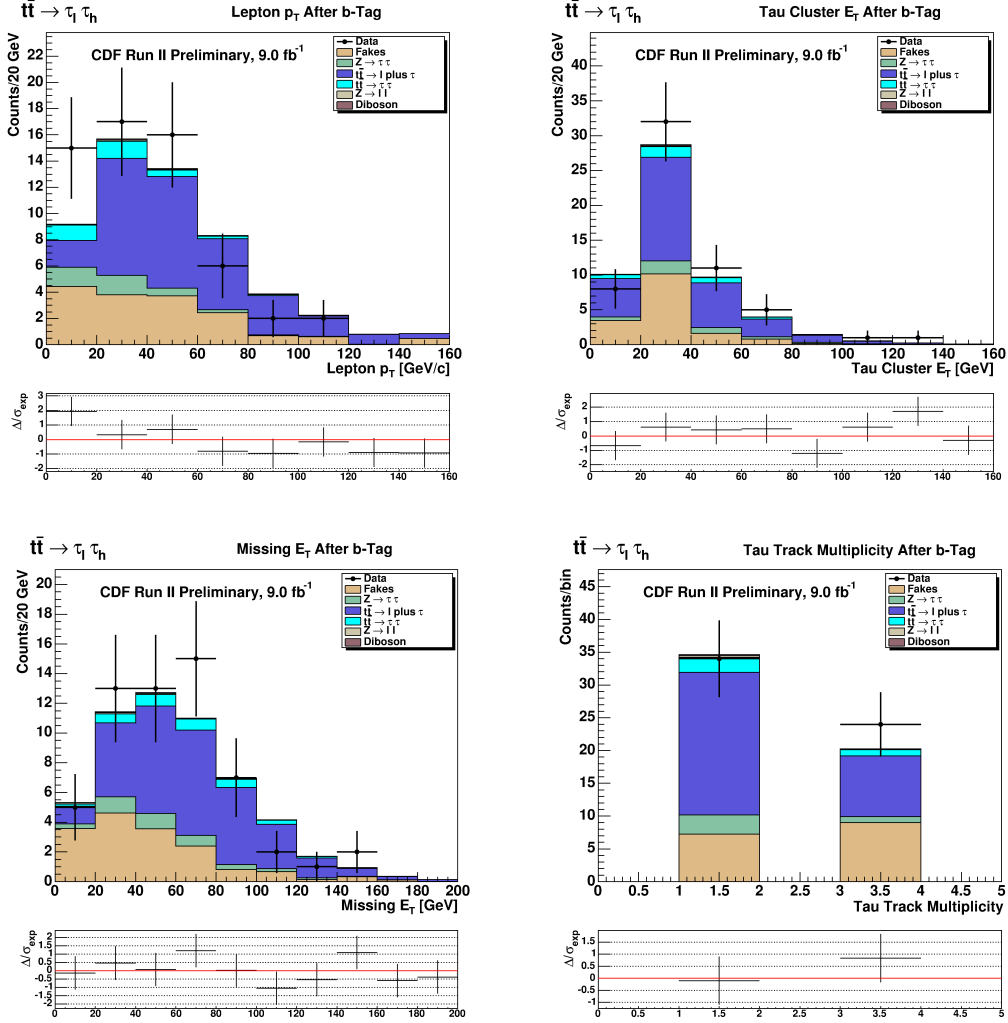
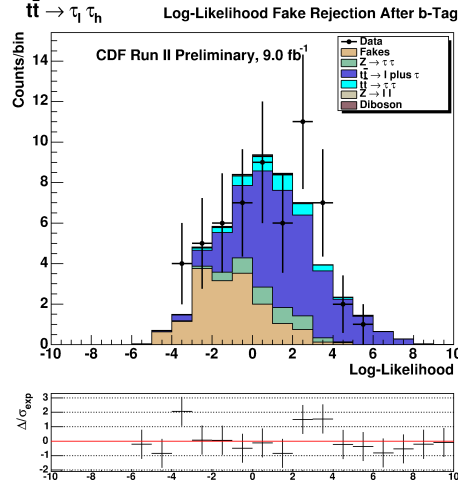


Figure 3: Distribution of electron E_T and muon p_T (top left), of tau cluster E_T (top right), \cancel{E}_T (top left), and track multiplicity of tau induced jet (top right).

We require $\ln(LR) > 0$ and the results obtained with the likelihood selection is summarized in Figure 5. It is possible to notice a significant reduction of the background with fake taus. Table III summarizes the uncertainty in the selection efficiency due the propagation of the systematic uncertainties, expressed in percentage.

We analyzed the propagation of the systematic uncertainties on the expected number of events after the LLR discrimination. The expected events from background and signal processes are summarized in Table IV, where we report the error induced by all the systematic uncertainties.

Figure 4: Validation plots of $\ln(LR)$ distribution using electron and muon samples.

$t\bar{t} \rightarrow \tau\ell\tau h + X$	Uncertainties of Final Selection					
	$Z/\gamma^* \rightarrow \tau\tau$	$Z/\gamma^* \rightarrow \ell\ell$	Diboson	$t\bar{t} \rightarrow \tau\ell + X$	$t\bar{t} \rightarrow \tau\tau + X$	fakes
Trigger	$\pm 3\%$	$\pm 3\%$	$\pm 3\%$	$\pm 3\%$	$\pm 3\%$	$\pm 3\%$
Cross Section	$\pm 15\%$	$\pm 15\%$	$\pm 6\%$	—	—	—
PDF	—	—	—	$\pm 0.5\%$	$\pm 0.5\%$	—
Showering	—	—	—	$\pm 3\%$	$\pm 3\%$	—
Color Recon.	—	—	—	$\pm 4\%$	$\pm 4\%$	—
ISR/FSR	—	—	—	$\pm 9\%$	$\pm 9\%$	—
Pile Up	—	—	—	$\pm 2.5\%$	$\pm 3\%$	—
JEC	$\pm 9\%$	$\pm 20\%$	$\pm 20\%$	$\pm 2\%$	$\pm 3\%$	—
τE_T scale	$\pm 4\%$	$\pm 20\%$	$\pm 20\%$	$\pm 0.5\%$	$\pm 1.5\%$	—
τ ID scale	$\pm 3\%$	—	$\pm 3\%$	$\pm 3\%$	$\pm 3\%$	—
SECVTX Tag	$\pm 5\%$	$\pm 5\%$	$\pm 5\%$	$\pm 5\%$	$\pm 5\%$	—
SECVTX Mistag	$\pm 20\%$	$\pm 20\%$	$\pm 20\%$	—	—	—
Fake Rate	—	—	—	—	—	$+7\%$ -20%

CDF Run II Preliminary, 9.0 fb^{-1} Table III: The summary table of the systematic uncertainties of the expected events passing the kinematic selection plus the requirements of one secondary vertex tag and $\ln(LR) > 0$. Values are expressed in percent.

IX. CROSS SECTION MEASUREMENT

The $t\bar{t}$ cross section is defined as:

$$\sigma_{t\bar{t}} = \frac{N_{sel} - \sum N_{bg}^i}{\sum_{CMX, CMUP, CEM} [(BR_{\ell\tau}\epsilon_{\ell\tau} + BR_{\tau\tau}\epsilon_{\tau\tau}) \int \mathcal{L} dt]} \quad (4)$$

where N_{sel} is the number of selected signal events of the lepton plus tau and ditau channel; N_{bg} is the number of expected background events; the sum extends over the lepton categories used in our analysis, namely the electron reconstructed with CEM detector and muon with CMUP and CMX muon chambers; $BR_{\ell\tau}$ represents the combinatory product of top quark decay branching ratio into electron or muon, $BR(t \rightarrow \ell\nu b)$, and top decay into hadronically decaying tau $BR(t \rightarrow \tau\nu b) \cdot BR(\tau \rightarrow \text{jet } \nu)$;

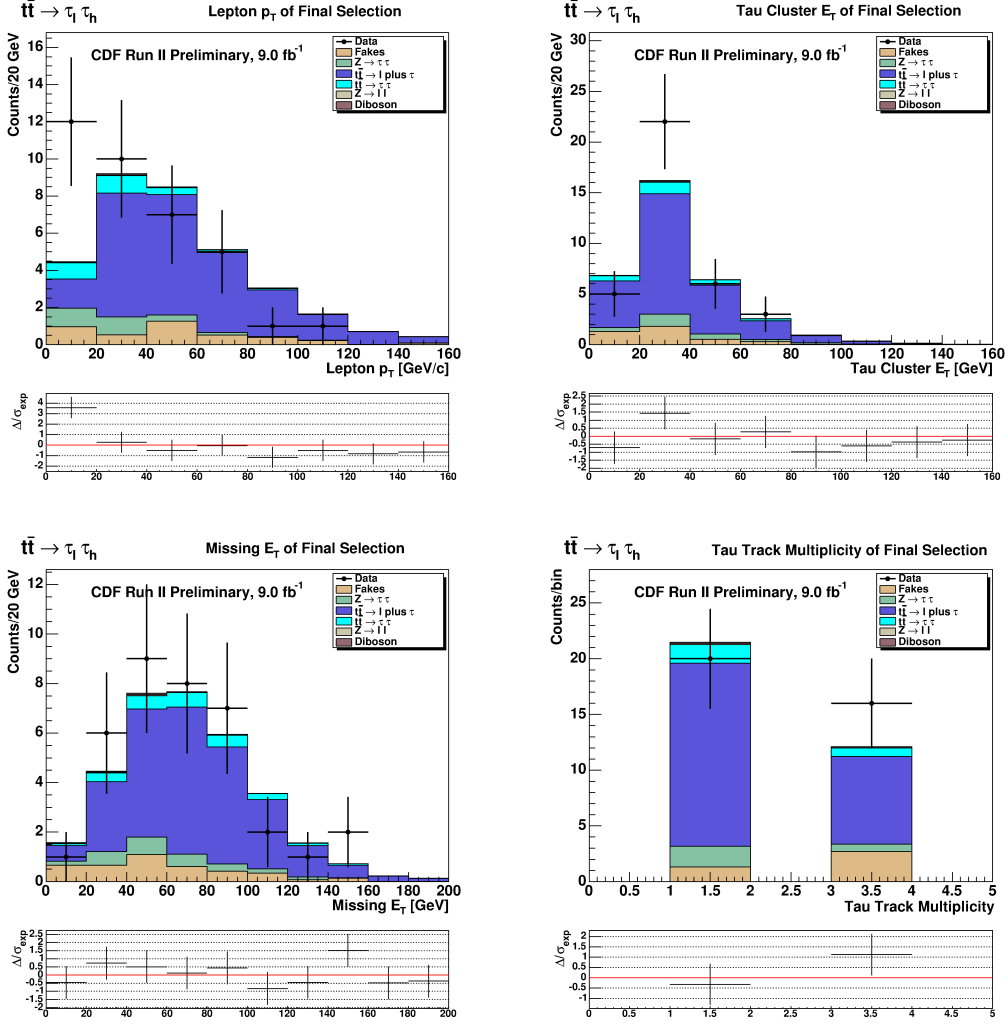


Figure 5: Distribution of electron E_T or muon p_T (top left), of tau cluster E_T (top right), \cancel{E}_T (bottom left), and track multiplicity of tau induced jet (bottom right). Results obtained with kinematic selection, one b -jet tagging and LLR discriminant.

$BR_{\tau\tau}$ is the branching ratio of top pair decay into leptonically decaying tau plus hadronically decaying tau; $\epsilon_{\ell\tau}$ and $\epsilon_{\tau\tau}$ are the overall selection efficiencies for the ditau and lepton plus tau channel.

To derive a $t\bar{t}$ cross section measurement we assume a 100% branching ratio of top into W and b and use the measured tau into electron or muon and hadrons branching ratios from the PDG [25]. We obtain a $t\bar{t}$ cross section of We propagate the systematic uncertainties that are summarized in Table III individually, correlated among channels within each source of uncertainty and uncorrelated among different uncertainties.

$$\sigma_{t\bar{t}} = 8.2 \pm 2.3(stat.)_{-1.1}^{+1.2}(syst.) \pm 0.5(lum.) \text{ pb.} \quad (5)$$

Our measurement of the $t\bar{t}$ cross section assuming Standard Model top decay is in good agreement with other combinations of all electron and muon channels from CDF, $\sigma_{t\bar{t}} = 7.5 \pm 0.5 \text{ pb}$ [23], and $D0$ measurements, $\sigma_{t\bar{t}} = 7.6 \pm 0.8 \text{ pb}$ [24].

$t\bar{t} \rightarrow \tau_\ell \tau_h + X$		Events of Final Selection	
Process	Muon Sample	Electron Sample	Total
Fakes	$1.80 \pm 0.31^{+0.13}_{-0.31}$	$2.20 \pm 0.64^{+0.18}_{-0.48}$	$4.01 \pm 0.71^{+0.31}_{-0.80}$
$Z/\gamma^* \rightarrow \tau\tau$	$1.12 \pm 0.07 \pm 0.25$	$1.41 \pm 0.08 \pm 0.29$	$2.53 \pm 0.11 \pm 0.53$
$Z/\gamma^* \rightarrow \ell\ell$	$0.10 \pm 0.03 \pm 0.03$	$0.03 \pm 0.01 \pm 0.01$	$0.13 \pm 0.03 \pm 0.04$
Diboson	$0.09 \pm 0.02 \pm 0.03$	$0.09 \pm 0.02 \pm 0.03$	$0.17 \pm 0.03 \pm 0.05$
$t\bar{t} \rightarrow \tau\ell + X$	$10.56 \pm 0.08 \pm 1.34$	$13.73 \pm 0.10 \pm 1.75$	$24.29 \pm 0.13 \pm 3.09$
$t\bar{t} \rightarrow \tau\tau + X$	$1.07 \pm 0.03 \pm 0.14$	$1.37 \pm 0.03 \pm 0.18$	$2.44 \pm 0.04 \pm 0.32$
Total Expected	$14.7 \pm 0.3^{+1.6}_{-1.7}$	$18.8 \pm 0.6^{+2.1}_{-2.1}$	$33.6 \pm 0.7^{+3.7}_{-3.8}$
Observed	12	24	36

CDF Run II Preliminary, 9.0 fb^{-1} Table IV: Expected events and data events passing the kinematic selection plus the requirements of one tight SECVTX tag and $\ln(LR) > 0$.

X. BRANCHING RATIO OF $t \rightarrow \tau\nu b$

The measurement of the $t \rightarrow \tau\nu b$ decay branching ratio is done using as signal the lepton plus tau event category. The procedure of evaluation is similar to the one of the previous section. The Branching ratio is given by the following equation:

$$BR(t \rightarrow \tau\nu b) = \frac{1}{2BR(W \rightarrow \ell\nu)} \frac{N_{sel} - \sum_i N_{bg}^i}{\sigma_{t\bar{t}} \sum_{CMX, CMUP, CEM} \epsilon_{\ell\tau} \int \mathcal{L} dt}. \quad (6)$$

We considered also the uncertainty of the measured top pair production cross section. We use the most recent CDF combination, 7.5 ± 0.5 [23]. We calculated the propagation of the systematics into the $BR(t \rightarrow \tau\nu b)$. The result is

$$BR(t \rightarrow \tau\nu b) = 0.120 \pm 0.030(stat.)^{+0.022}_{-0.019}(syst.) \pm 0.007(lum.), \quad (7)$$

in good agreement with the SM prediction on the top decay process $t \rightarrow Wb$ and the branching ratio values of W boson leptonic decay fitted by the Particle Data Group [25]:

$$BR(W \rightarrow \ell\nu) = (10.80 \pm 0.09) \% (\text{average over } e, \mu, \tau \text{ decay modes}). \quad (8)$$

Our measurement of the branching ratio $BR(t \rightarrow \tau\nu b)$ indicates that we may limit the branching ratio $BR(t \rightarrow H^\pm b)$, since in the MSSM picture the $H^\pm \rightarrow \tau\nu$ is favourite for $\tan(\beta) > 1$ and $M_{H^\pm} < M_t$.

XI. SINGLE AND DI-TAU COMPONENT DISCRIMINANT

To discriminate the signature of the lepton plus tau decay from the ditau processes and perform a measurement of the branching ratio of top quark decay in tau, we implemented a second log-likelihood ratio (we report as LLR') discriminant method to separate the two processes. We use the distribution of the transverse mass of the electron (or muon) plus \cancel{E}_T ; the azimuthal angle between electron and \cancel{E}_T ; the electron (or muon) transverse energy (momentum).

The templates used are obtained with sample of events from MC simulation. We require the kinematic selection, at least one tight SECVTX tag and $\ln(LR) > 0$. We represent in Figure 6 the distribution along $\ln(LLR')$ of data events compared with the expectations.

A. Likelihood Fit to Data

We use the MClimit package [26] to fit the event expectation to the data event distribution and extract the branching ratio $BR(t \rightarrow \tau\nu b)$. The branching ratio is an unconstrained parameter of the fit. The

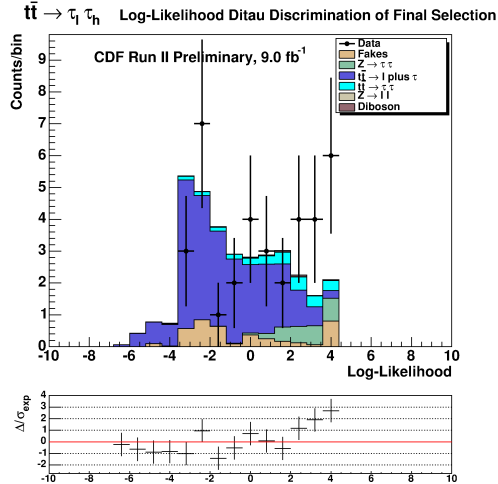


Figure 6: Comparison of data and expectation distribution along $\ln(LR')$ using electron and muon samples.

top pair contribution in the lepton plus tau and the di-tau decay channels are set respectively to be linearly and quadratically dependent on the parameter $BR(t \rightarrow \tau\nu b)$. The systematic uncertainties of the counting experiment are used as nuisance parameters of the fit. The top pair cross section measurement from the CDF combination is used to constrain the top pair contribution. Its uncertainty is used as rate systematic for the fit.

The result of the fit is:

$$BR(t \rightarrow \tau\nu b) = 0.098 \pm 0.022(stat.) \pm 0.014(syst.) \quad (9)$$

From the fit it is possible to obtain also the upper limit of the branching ratio of top into tau. This limit is fundamental to constrain the decay of top pair into charged Higgs in the hypothesis that the mass of the charged Higgs is lower than the top quark mass.

For this measurement we repeated the fit of the expected distributions to data rescaling the MC expectations of signal top events on the base of the branching ratio. The lepton plus tau channel and the di-tau channel scale linearly and quadratically respectively with the $BR(t \rightarrow \tau\nu b)$. We obtain

$$BR(t \rightarrow \tau\nu b) < 0.159 \text{ at } 95\% \text{ C.L.} \quad (10)$$

XII. CONCLUDING REMARKS

The study reported in this thesis is motivated by a twofold purpose. In first place a measurement of a poorly known top pair decay channels into tau. The study of this decay channels have been so far limited by small branching ratios and by the high background of jets misidentified as taus. In second place the search for phenomena beyond the Standard Model in the study of the third generation of fermions (both top quark and tau lepton).

With the full CDF data sample we obtain the most precise measurement on the dileptonic channel with one hadronic tau decay. The measurement is in good agreement with the tevatron combination

and theoretical expectations.

-
- [1] CDF Collaboration, “The CDF II Detector Technical Design Report”, FERMLAB-PUB-96/390-E (1996).
 - [2] A. Affolder et al., “COT Central Outer Tracker”, Nucl. Instrum. Meth. **A526**, 249 (2004).
 - [3] N. Timothy, “The CDF L00 Detector”, CDF Public Note 5780 (2001).
 - [4] A. Sill, “CDF Run II Silicon Tracking Project”, Nucl. Instrum. Meth. **A447**, 1 (2000).
 - [5] A. Affolder et al., “Status Report of the Intermediate Silicon Layer Detector at CDF II”, Nucl. Instrum. Meth. **A485**, 178-182 (2002).
 - [6] C. M. Ginsburg et al., “CDF Run II Muon System”, Eur. Phys. J. **C33**, S1002 (2004).
 - [7] D. Acosta et al., “The Performance of the CDF Luminosity Monitor”, Nucl. Instrum. Methods **A494**, 57-62 (2002).
 - [8] R.J. Tesarek et al., Nucl. Inst. and Meth. **A514** (2003) 188.
 - [9] P. Dong et al., *CDF internal note* 8219, 2006.
 - [10] G. Lindström, M. Moll and E. Fretwurst, Nucl. Instr. and Meth. **A426** (1999) 1.
 - [11] C. Cuenca Almenar, “Search for the Neutral MSSM Higgs Bosons in the Tau-Tau Decay Channels at CDF Run II”, PhD Thesis, Universitat de Valencia (2008).
 - [12] A. Anastassov et al., “Search for Neutral MSSM Higgs Boson(s) in the Tau Tau Decay Channel”, CDF internal note, CDF/PHYS/EXOTIC/CDFR/8972 (2007).
 - [13] CDF Collaboration, “Search for Neutral MSSM Higgs Bosons Decaying to Tau Pairs with 1.8 fb^{-1} of Data”, CDF public note, CDF/PHYS/EXOTIC/PUBLIC/9071 (2007)
 - [14] P. Murat, Y. Tu, “Monte Carlo modelling of the jet $\rightarrow \tau_h$ fake rates, CDF/DOC/ELECTROWEAK/CDFR/8809 (2007).
 - [15] D. Acosta et al., Phys. Rev. D71, 052003 (2005)
 - [16] S. Rolli et al., “Electron id efficiencies and scale factors for periods 9 to 12”, CDF/DOC/ELECTRON/CDFR/9148 (2007).
 - [17] X.Zhang et al., “High-pT muons recommended cuts and efficiencies for summer 2006”, CDF/ANAL/TOP/CDFR/8262 (2006).
 - [18] S. Camarda et al., “Measurement of $Z/\gamma^* \rightarrow e^+e^- + \text{jets}$ Production Cross Section”, CDF/PHYS/JET/PUBLIC/10394 (2011).
 - [19] A. Anastassov et al., “Search for Neutral MSSM Higgs Boson(s) in the Tau Tau Decay Channel”, CDF/ANAL/EXOTIC/CDFR/7622 (2005).
 - [20] H. L. Lai et al., “Global QCD Analysis of Parton Structure of the Nucleon: CTEQ5 Parton Distributions”, Eur. Phys. J. **C12**, 375-392 (2000).
 - [21] J. Campbell and K. Ellis, “Monte Carlo for FeMtobarn processes”, [shttp://mcfm.fnal.gov](http://mcfm.fnal.gov).
 - [22] J. Campbell and K. Ellis, “Update on vector boson pair production at hadron colliders”, Phys. Rev. **D60**, 113006 (1999).
 - [23] CDF Collaboration, “Combination of CDF top quark pair production cross section measurements with up to 4.6 fb^{-1} ”, CDF Conference note 9913 (2009).
 - [24] D0 Collaboration, “Measurement of the $t\bar{t}$ production cross section using dilepton events in $p\bar{p}$ collisions”, Phys. Lett. **B**, 704, 403-410 (2011).
 - [25] K. Nakamura et al. (Particle Data Group), J. Phys. G 37, 075021 (2010).
 - [26] T. Junk, “Sensitivity, Exclusion and Discovery with Small Signals, Large Backgrounds, and Large Systematic Uncertainties”, CDF note CDF/DOC/STATISTICS/PUBLIC/8128.